

Scientific paper

The Effect of Fluoride Ions on the Corrosion Behaviour of Ti Metal, and Ti6–Al–7Nb and Ti–6Al–4V Alloys in Artificial Saliva

Ingrid Milošev,^{1,*} Barbara Kapun¹ and Vid Simon Šelih²

¹ Jožef Stefan Institute, Department of Physical and Organic Chemistry, Jamova 39, SI-1000, Ljubljana, Slovenia

² National Institute of Chemistry, Analytical Chemistry Laboratory, Hajdrihova 19, SI-1000 Ljubljana, Slovenia

* Corresponding author: E-mail: ingrid.milosev@ijs.si;

Tel.: + 386 1 4773 452

Received: 30-07-2012

Paper submitted for the Special Issue of the Acta Chimica Slovenica dedicated to Professor Boris Žemva.

Abstract

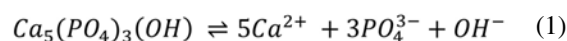
Metallic materials used for manufacture of dental implants have to exhibit high corrosion resistance in order to prevent metal release from a dental implant. Oral cavity is aggressive towards metals as it represents a multivariate environment with wide range of conditions including broad range of temperatures, pH, presence of bacteria and effect of abrasion. An increasing use of various Ti-based materials for dental implants and orthodontic brackets poses the question of their corrosion resistance in the presence of fluoride ions which are present in toothpaste and mouth rinse. Corrosion behaviour of Ti metal, Ti–6Al–7Nb and Ti–6Al–4V alloys and constituent metals investigated in artificial saliva is significantly affected by the presence of fluoride ions (added as NaF), as proven by electrochemical methods. Immersion test was performed for 32 days. During that time the metal dissolution was measured by inductively coupled plasma mass spectrometry. At the end of the test the composition, thickness and morphology of the surface layers formed were investigated by X-ray photoelectron spectroscopy and scanning electron microscopy.

Keywords: Dental alloys; artificial saliva; corrosion; X-ray photoelectron spectroscopy; ICP-MS

1. Introduction

A connection between fluoride and inhibition of caries was recognized in the 1930s.¹ In the 1940s the U.S. Public Health service developed recommendation for fluorination of public water supplies which, in time, led to the development of dental product containing fluoride like toothpaste, mouth rinses and gels. In Europe, public water supplies are only rarely fluorinated. Instead, regular fluorination for children in schools is used as a prevention measure for caries development.² Dental caries is an infectious, transmissible disease in which bacterial by-products (i.e., acids) dissolve the hard surfaces of teeth. Carious lesion initiates when cariogenic bacteria in dental plaque metabolize a substrate from the diet (e.g., sugars and other fermentable carbohydrates) and the acid produced as a metabolic by-product demineralizes the adjacent enamel crystal surface. Demineralization involves the loss of cal-

cium, phosphate, and carbonate from hydroxyapatite, $\text{Ca}_5(\text{PO}_4)_3\text{OH}$. These minerals can be captured by surrounding plaque and be available for reuptake by the enamel surface. Fluoride, when present in the mouth, is also retained and concentrated in plaque. It inhibits the demineralization of sound enamel and enhances the remineralization of demineralized enamel. De-mineralized enamel takes up the released fluoride thus leading to establish an improved enamel crystal structure and formation of fluoroapatite instead of hydroxyapatite³:



This improved structure is more acid resistant and contains more fluoride and less carbonate. Applying fluoride gel or other products containing a high concentration

of fluoride to the teeth leaves a temporary layer of calcium fluoride-like material available to remineralize enamel. The wide variations in fluoride intake are reported in literature, as recently reviewed.² The average daily intake of fluoride in children (age 4–8 years) from diet, fluoride supplements and use of fluorinated dental products in non-fluorinated areas is on average 0.067 (range, 0.034–0.097) mg/day/kg body weight, and in fluorinated area on average 0.066 (range, 0.019–0.139) mg/day/kg body weight.² Out of 0.067 mg/day/kg body weight in non-fluorinated areas, on average 0.025 mg/day/kg body weight originates from diet, 0.034 mg/day/kg body weight from fluoride supplements, and 0.008 mg/day/kg body weight from toothpaste.² Out of 0.066 mg/day/kg body weight in fluorinated areas, on average 0.058 mg/day/kg body weight originates from diet, and 0.008 mg/day/kg body weight from toothpaste.² Therefore, in non-fluorinated areas the majority of fluoride intake originates from fluoride supplements, while in fluorinated areas the majority of fluoride intake originates from diet.

There exist many debates concerning the effectiveness of fluoride treatments including criticism of water fluorination being compulsory medication since no proof exists that it decrease caries by systemic fluoride intake into body and it is effective only while present in mouth, fluoride in higher amounts causes dental fluorosis, it is toxic and may cause allergies, it cumulatively accumulates in bone and may lead to osteoporosis and cancer, etc. Last but not least, it has been reported that fluoride ions promote the corrosion of dental implants. The aim of the present work is to investigate this matter more closely using a variety of methods.

Dental materials must exhibit suitable physical and mechanical properties but also high corrosion resistance. The release of metal ions may cause local tissue responses, such as gingival swelling, mucosal pain, etc.^{4,5,6} It was published recently that cell proliferation (72-h observation) determined by MTT (dimethylthiazol-diphenyl tetrazolium bromide) measurements was decreased significantly only for NaF-treated samples of titanium; protein content assay experiments showed no such effect.⁷ The authors emphasized that epithelial cell culturing results can depend on the method used, and the adverse effect of a high F⁻ concentration and low pH should be considered when prophylactic gels are applied by patients with titanium implants.⁷ Among other dental materials, stainless steel, CoCr-based and Ti-based alloys have been used for the manufacture dental implants and orthodontic products.⁸ It has been reported recently that electrochemical methods in combination with chemical methods are well suitable for classification of metals and alloys according to their corrosion resistance.⁵ While Au-Pt and Au-Ag alloys released high quantity of metallic ions, Ti metal released no metal ions.⁵ High corrosion resistance of titanium in artificial saliva has been recognized to be due to the formation of protec-

tion TiO₂ layer formed on its surface.⁹ Due to recent restriction of use of nickel in manufactured product that come into contact with skin and other tissue the use of stainless steel in dental products is limited¹⁰. Instead, Ti-based materials are increasingly used. Besides corrosion resistance, the addition of alloying elements like niobium improves also the mechanical properties of titanium, e.g. ultimate tensile strength.¹¹ Although titanium and its alloys are highly corrosion resistant under simulated physiological conditions,^{12,13} their protectiveness may be endangered by the presence of fluoride ions.^{14,15,16,17,18} The corrosion process is especially pronounced in acidic environment.^{7,19,20}

Regarding the increased use of Ti and its alloys for manufacture of dental implants and parts of orthodontic brackets, in this study we aimed to address this problem in detail using electrochemical technique of potentiodynamic polarization measurements and biodegradation tests performed using inductively coupled plasma – mass spectroscopy (ICP-MS) for the measurement of metal ion release, X-ray photoelectron spectroscopy (XPS) for the analysis of thickness and composition, and scanning electron microscopy (SEM) combined with chemical analysis (EDS) for the analysis of surface morphology.

2. Experimental

2.1. Materials and Solutions

Three titanium-based materials were used in this study. **Titanium** metal (purity 99.6%, annealed) and **Ti-6Al-4V** alloy (Ti90/Al6/V4; annealed) were supplied by Goodfellow (Cambridge Ltd., UK). Samples of **Ti-6Al-7Nb** alloy were cut from the femoral component of the total hip replacement manufactured by company Sulzer (Winthertur, Switzerland). Individual alloy metal components of the alloys were also investigated: **aluminium** (purity 99.0%), **niobium** (purity 99.9%) and **vanadium** (purity 99.8%) all supplied by Goodfellow (Cambridge Ltd., UK). Individual metals and Ti-6Al-4V were purchased in the shape of a 2 mm-thick foil. Samples were cut from the foil or component in the shape of discs with 15 mm diameter for electrochemical and XPS measurements, and in the shape of plates with 1 cm × 5 cm dimension.

The samples were mechanically ground under water successively with 320, 500, 800, 1.000, 1.200, 2.400 and 4.000 – grit SiC papers. Each sample was ground in one direction until all imperfections were removed and the surface was covered with a uniform pattern of scratches. Samples were cleaned with ethanol in an ultrasonic bath for two minutes, double-rinsed with Milli-Q water, and finally dried in a stream of nitrogen.

Measurements were performed in artificial saliva (AS), with the composition given in Table 1. The pH was adjusted to 5.3 by the addition of HCl (1M) solution. All

chemicals used for the preparation of solutions were of *p.a.* purity supplied by Kemika (Zagreb, Croatia), and Carlo Erba Reagents (Rodano, Italy). Sodium fluoride supplied by Sigma Aldrich was added to artificial saliva in the concentration of 0.25%.

Table 1. Chemical composition of artificial saliva.²¹

Compound	Concentration (g/L)
NaCl	0.4
KCl	0.4
CaCl ₂ · 2H ₂ O	0.795
NaH ₂ PO ₄ · 2H ₂ O	0.69
Na ₂ S · 9H ₂ O	0.005
urea	1.0

2. 2. Electrochemical Measurements

Electrochemical measurements were performed in a three-electrode corrosion cell (volume 300 mL, Autolab, Ecochemie, Netherlands) at a temperature of 37 ± 0.1 °C. A specimen embedded in a Teflon holder, with an area of 0.785 cm² exposed to the solution, served as the working electrode. A saturated calomel electrode (SCE, 0.2415 V vs. saturated hydrogen electrode, SHE) was used as reference electrode and carbon rods as counter-electrode. The reference electrode was connected to the cell *via* a Luggin probe. Measurements were carried out with an Autolab PGSTAT 12 potentiostat/galvanostat (Metrohm Autolab, Utrecht, The Netherlands) controlled by Nova 1.7 software. The corrosion parameters were calculated by this software based on the Stern–Geary equation.²²

Prior to measurements, the samples were allowed to stabilize for 1h under open circuit conditions. The stable, quasi-steady state potential reached at the end of the stabilization period is denoted as the corrosion potential, E_{corr} . Potentiodynamic measurements were performed using a 1 mV/s potential scan rate, starting at 250 mV negative to E_{corr} and then increased in the anodic direction.

2. 3. Measurements of Concentration of Released Metal Ions

Sample of titanium, Ti–6Al–7Nb and Ti–6Al–4V plates were prepared as described in section 2.1. They were immersed in 100 mL glass containers containing artificial saliva (AS) and artificial saliva containing NaF (AS+NaF). Containers were placed in a thermostat bath and the temperature maintained at 37 ± 0.1 °C. The immersion test lasted for 32 days. Each experiment was performed in duplicate. Glass containers with only AS and AS+NaF served as blank samples. The experimental conditions were as for the test samples.

In order to follow the biodegradation of alloys, the concentrations of dissolved metal ions (Ti, Nb, Al and V) in AS and AS+NaF were measured using inductively coupled

plasma – mass spectroscopy (ICP-MS). During the immersion period, 1 mL of solution aliquot was taken from each solution after the following immersion periods: 7, 14, 21, 28 and 32 days. The aliquot was added to a polypropylene tube (Sarstedt, Nümbrecht, Germany) containing 1 mL 2% HNO₃ solution and stored for ICP-MS analysis.

Concentrations of dissolved ions were measured using an Agilent 7500ce ICP-MS instrument (Agilent Technologies, Palo Alto, USA) equipped with MicroMist pneumatic nebulizer and a peltier-cooled spray chamber. 1500 W RF power was used. Ar carrier and make-up gas was used at 0.85 and 0.2 L min⁻¹, respectively. Octopole reaction system (ORS) in kinetic energy discrimination mode with 5 mL min⁻¹ of He collision gas was used to reduce the effect of polyatomic interferences from the sample matrix. To further reduce the influence of matrix, a method of standard additions was used for calibration (11 points). Results were expressed as mean concentrations (c_{avg}) in g L⁻¹ of duplicate measurements \pm standard deviation (σ). The concentrations of metal ions measured in blank samples were subtracted from the concentrations measured in test samples. Limit of detection (LOD) was calculated as three-fold standard deviation of replicate blank measurements. In some cases (niobium and vanadium) the instrumental LOD was taken in the account. The following values of LOD were determined in artificial saliva: 41 µg/L for Al, 0.21 µg/L for Ti, 0.009 µg/L for Nb, and 0.032 µg/L for V. The following values of LOD were determined in artificial saliva containing 0.25% NaF: 241 µg/L for Al, 3.37 µg/L for Ti, 1.4 µg/L for Nb, and 0.07 µg/L for V.

2. 4. X-ray Photoelectron Spectroscopy

X-ray photoelectron spectroscopy (XPS) was performed with a TFA Physical Electronics Inc. spectrometer using non- and mono-chromatized Al K_α radiation (1486.6 eV) and a hemispherical analyzer. The mono-chromatized radiation used for high-resolution spectra yields a resolution of 0.6 eV, as measured on an Ag 3d_{5/2} peak. These spectra were used to differentiate between various species, whereas spectra obtained, using the non-monochromatized variation, were used for quantifying the chemical composition. The take-off angle used, defined as the angle of emission relative to the surface, was 45°. The energy resolution was 0.5 eV. Survey scan spectra were recorded at a pass energy of 187.85 eV, and individual high-resolution spectra at a pass energy of 23.5 eV with an energy step of 0.1 eV. After taking the surface spectra, depth profiling of the oxidized layers was performed. An Ar⁺ ion beam, with an energy level of 3 keV and a raster of 4 mm × 4 mm (sputter rate 1.7 nm/min determined on the SiO₂ standard) was used for sputtering.²³

The 2p_{3/2} peak for Ti metal state is centred at 454.2 eV, and that for Ti in oxidized state at 459.2 eV. The cen-

tre of the Al $2p_{3/2}$ peak in aluminium metal is centred at 71.5 eV, whilst in the Al_2O_3 it is located at 74.8 eV.^{12,13} The centre of the Nb $3d_{5/2}$ peak of metallic niobium appears at 203.5 eV. Niobium can form oxides in various oxidation states, *i.e.*, NbO, NbO₂ and Nb₂O₅. The binding energy increases with increasing oxidation state, *i.e.* from 204.5 eV for NbO and NbO₂, to 207.5 – 207.8 eV for Nb₂O₅.¹³ The position of the centre of the O 1s peak depends on the hydration of the layer and ranges from 530.1 eV (oxide component, O²⁻) and 531.2 eV (hydroxide component, OH⁻) to 532.2 eV (water, H₂O, and phosphate containing species, PO₄³⁻).

2. 4. Scanning Electron Microscopy

A scanning electron microscopy (SEM) Joel JSM-5800 and an energy dispersive X-ray spectrometer (EDS) Oxford Instruments - Link ISIS 3000 were used to analyse the morphology of sample surface.

3. Results and Discussion

3. 1. Electrochemical Measurements

Anodic polarization curves were recorded for Ti metal and Ti-6Al-7Nb and Ti-6Al-4V alloys in artificial saliva (AS) with and without addition of 0.25% NaF (Figs. 1a,b). Corrosion parameters, corrosion potential, E_{corr} , and corrosion current density, j_{corr} , were determined by the analysis of Tafel range. The values of E_{corr} are most negative for the Ti-6Al-4V alloy and shift to more positive values for Ti-6Al-7Nb and Ti (Table 2). At the same time the values of j_{corr} decrease being the lowest for Ti and the highest for the Ti-6Al-4V alloy. These data indicate that titanium exhibits the best corrosion performance in the range close to the corrosion potential relevant for general corrosion. Following the Tafel region the first current density plateau forms indicating the passivity of all three materials investigated. At approximately 1.0 V the current density starts to increase again and is followed by the formation of the second current density plateau which extends from 2.0 V to high anodic potentials. These curves recorded in artificial saliva are similar to those recorded in simulated physiological solution.^{9,12,13,24,25,26,27} In the first current density plateau titanium(IV) oxide containing sub-oxides (TiO and Ti₂O₃) is formed. The second current density plateau is established due to complete transformation to TiO₂ resulting in the passivity of the surface. The layer formed is highly protective as the current density remains independent on potential in a broad potential region. For Ti and Ti-6Al-7Nb the passive range extends to high anodic potential of 6 V, while for the Ti-6Al-4V alloy it is narrower. At 3.3 V the current density starts to increase abruptly due to the localized corrosion process and breakdown of the passive layer leading to pitting corrosion. Therefore, in terms of corrosion resi-

stance in artificial saliva, Ti and the Ti-6Al-7Nb alloy exhibit similar behaviour with highly protective character, whilst the Ti-6Al-4V alloy is less protective towards localized corrosion. The current density is the lowest for Ti and the highest for the Ti-6Al-4V alloy in the whole potential region studied (Fig. 1). It is noteworthy that the value of breakdown potential of the Ti-6Al-4V alloy in simulated physiological solution (pH = 7.4) was determined as 3.5 V, *i.e.* not significantly different from the present work (pH = 5.3) again confirming that the pH value does not affect significantly the behaviour of Ti-based alloys.²⁶

The higher susceptibility of the Ti-6Al-4V alloy to localized passivity breakdown than that of Ti may be explained by the presence of the alloying elements, aluminium and vanadium, which both show a narrower potential range of stability (Fig. 2a) than titanium. Vanadium and aluminium show no tendency to passivity in artificial saliva, as evident by the progressive increase in current density at potentials more positive than E_{corr} . Their presence obviously plays an important role in the stability of the passive film and is detrimental in terms of resistance to pitting corrosion at high positive potentials.^{12,24} On the other hand, the Ti-6Al-7Nb alloy contains aluminium and

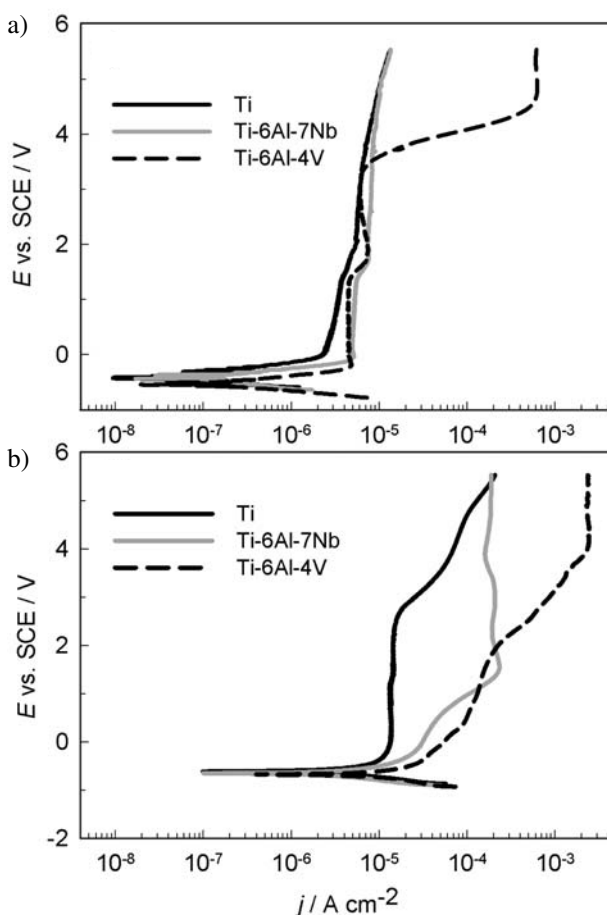
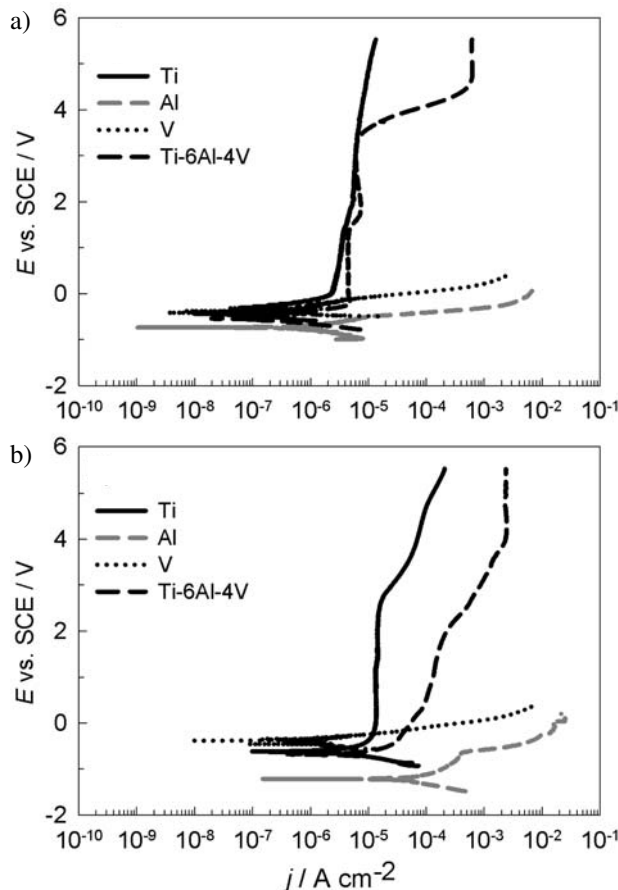
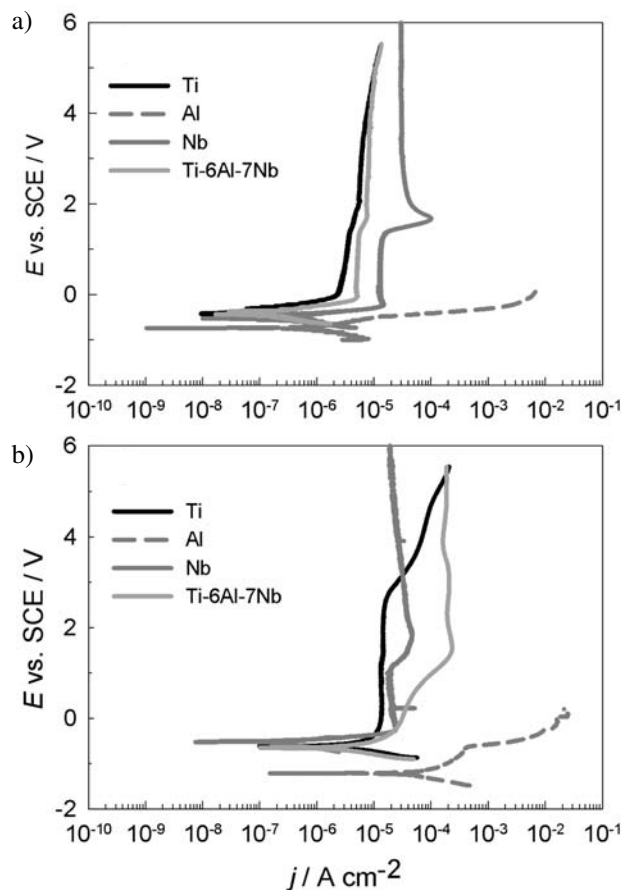


Figure 1. Potentiodynamic curves recorded for Ti, Ti-6Al-7Nb and Ti-6Al-4V in (a) artificial saliva and (b) artificial saliva containing 0.25% NaF. $dE/dt = 1$ mV/s.

Table 2. Values of corrosion potential, E_{corr} , and corrosion current density, j_{corr} , deduced from the potentiodynamic polarization curves presented in Fig. 1.

Material	Corrosion parameters			
	Artificial saliva		Artificial saliva + 0.25% NaF	
	$E_{\text{corr}} / \text{V}$	$j_{\text{corr}} / \text{A cm}^2$	$E_{\text{corr}} / \text{V}$	$j_{\text{corr}} / \text{A cm}^2$
Ti	-0.40	$5.0 \cdot 10^{-8}$	-0.62	$1.2 \cdot 10^{-6}$
Ti-6Al-7Nb	-0.43	$9.0 \cdot 10^{-8}$	-0.65	$1.8 \cdot 10^{-6}$
Ti-6Al-4V	-0.54	$1.2 \cdot 10^{-7}$	-0.69	$4.0 \cdot 10^{-6}$

**Figure 2.** Potentiodynamic curves recorded for the Ti-6Al-4V alloy and its individual metal components titanium, aluminium and vanadium in (a) artificial saliva and (b) artificial saliva containing 0.25% NaF. $dE/dt = 1 \text{ mV/s}$.**Figure 3.** Potentiodynamic curves recorded for the Ti-6Al-7Nb alloy and its individual metal components titanium, aluminium and niobium in (a) artificial saliva and (b) artificial saliva containing 0.25% NaF. $dE/dt = 1 \text{ mV/s}$.

niobium, the latter exhibiting excellent corrosion resistance in artificial saliva, superior to even that of titanium metal (Fig. 3a). Its presence in the alloy therefore acts beneficially resulting in the better corrosion performance compared to the Ti-6Al-4V alloy.

The addition of 0.25% NaF induces significant changes in the polarization curves (Fig. 1b) and deduced corrosion parameters (Table 2). The values of E_{corr} shift for approximately 200 mV more negative. At the same time the j_{corr} values increase for more than one order of magnitude (Table 2). The current density is increased compared to pure artificial saliva. For Ti, the first current

density plateau is established and extends up to approximately 3 V when the current density starts to increase. Similar behaviour, but with approximately one order of magnitude higher values, is observed for the Ti-6Al-4V alloy. The curve for the Ti-6Al-7Nb alloy is located between the curves for Ti and the Ti-6Al-4V alloy. The current density increases compared to plain artificial saliva but remains constant with increasing potential. Evidently, the addition of NaF to artificial saliva leads to a decreased corrosion resistance of all three Ti-based materials.

Polarization curves recorded for the two alloys and their individual metal components in artificial saliva con-

taining NaF are presented (Figs. 2b, 3b). While titanium, aluminium and vanadium showed worse corrosion behaviour in the presence of fluoride ions (Fig. 2b), niobium seems not to be significantly affected and the curve remains virtually unchanged (Fig. 3b). This behaviour is reflected in the behaviour of the Ti–6Al–7Nb alloy. Although increased compared to plain artificial saliva, the current density remains relatively constant up to high anodic potential.

Presented data show that the presence of fluoride ions leads to degradation of the passive layer on titanium-based samples even in a slightly acidic solution of artificial saliva (pH 5.3). Literature data confirmed that a decrease in the pH value to 4.2¹⁹, 2.5¹⁵ and 2.0¹⁸ induced further activation of titanium due to the shift of the potential below the equilibrium value for the reaction $\text{Ti}^{2+} \rightarrow \text{TiO}_2$. Consequently, the dissolution of titanium increased.

3. 2. Immersion Test

Samples of Ti, Ti–6Al–7Nb and Ti–6Al–4V were immersed in artificial saliva with and without addition of NaF for 32 days. During that time the concentration of ions dissolved in the solution was measured by inductively coupled plasma mass spectrometry (ICP-MS), whilst at the end of the test the composition and thickness of the surface layers were analysed by X-ray photoelectron spectroscopy (XPS), and their morphology by scanning electron microscopy (SEM) equipped with chemical analysis (EDS).

3. 2. 1. Concentration of Dissolved Ions

The quantity of titanium released from the three Ti-based materials in artificial saliva is similar (Fig. 4). It increases with immersion time and after 32 days reaches 30 $\mu\text{g/L}$ for Ti–6Al–7Nb alloy and only 10 $\mu\text{g/L}$ for Ti and Ti–6Al–4V alloy (Fig. 4a). These low concentrations pro-

ve that in artificial saliva all three materials exhibits low tendency to corrosion. The addition of NaF, however, increases the concentrations of dissolved titanium for three orders of magnitude (Fig. 4b). After 32 days of immersion the values range between 45.74 mg/L for the Ti–6Al–4V alloy and 86.36 mg/L for Ti–6Al–7Nb alloy. Takemoto *et al.* also observed an increased dissolution of titanium in 0.9% NaCl + 0.9% NaF solution. The addition of fluoride ions promotes the increased dissolution of other elements in the alloys. Aluminium dissolved in much larger quantity than titanium (Figs. 5a,b). This is the consequence of low aluminium corrosion stability in artificial saliva, as shown in section 3.1. (Figs. 2 and 3). After 32 days of immersion the concentration of Al reaches 816 $\mu\text{g/L}$ and 1231 $\mu\text{g/L}$ for Ti–6Al–4V and Ti–6Al–7Nb alloy, respectively, i.e. one order of magnitude larger than the concentration of titanium. In the presence of fluoride ions the concentration of Al increases approximately three-fold. Both niobium and vanadium dissolve in small quantity in artificial saliva (Figs. 5a,b); however, their concentration increases considerably, approximately for two orders of magnitude, in the presence of fluoride ions (Figs. 5c,d).

3. 2. 2. Composition and Thickness of Surface Layers

The chemical composition of the surface is deduced based on the X-ray photoelectron (XPS) survey spectra (Table 3). The surface contains abundant carbon content due to air contamination during the transfer of the sample from the cell to the XPS chamber. The layer is mainly comprised of titanium and oxygen confirming that titanium oxide is the major component of the layer formed during immersion of Ti, Ti–6Al–7Nb and Ti–6Al–4V in artificial saliva with or without fluoride ions present. In the case of alloys the oxide layer formed contains also minor elements. Besides Ti and O, the layer formed on Ti–6Al–7Nb contains minor elements aluminium and ni-

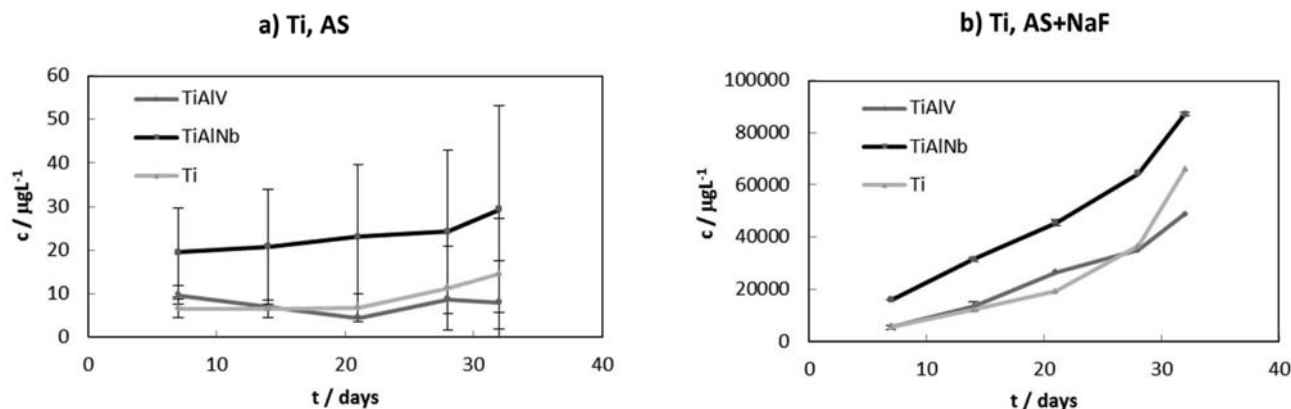


Figure 4. Concentration of titanium dissolved from Ti, Ti–6Al–7Nb and Ti–6Al–4V during 32 days immersion in (a) artificial saliva and (b) artificial saliva containing 0.25% NaF measured by ICP-MS. Symbols and bars represent mean values and standard deviation, respectively. In some cases bars are hardly visible due to small value of standard deviation.

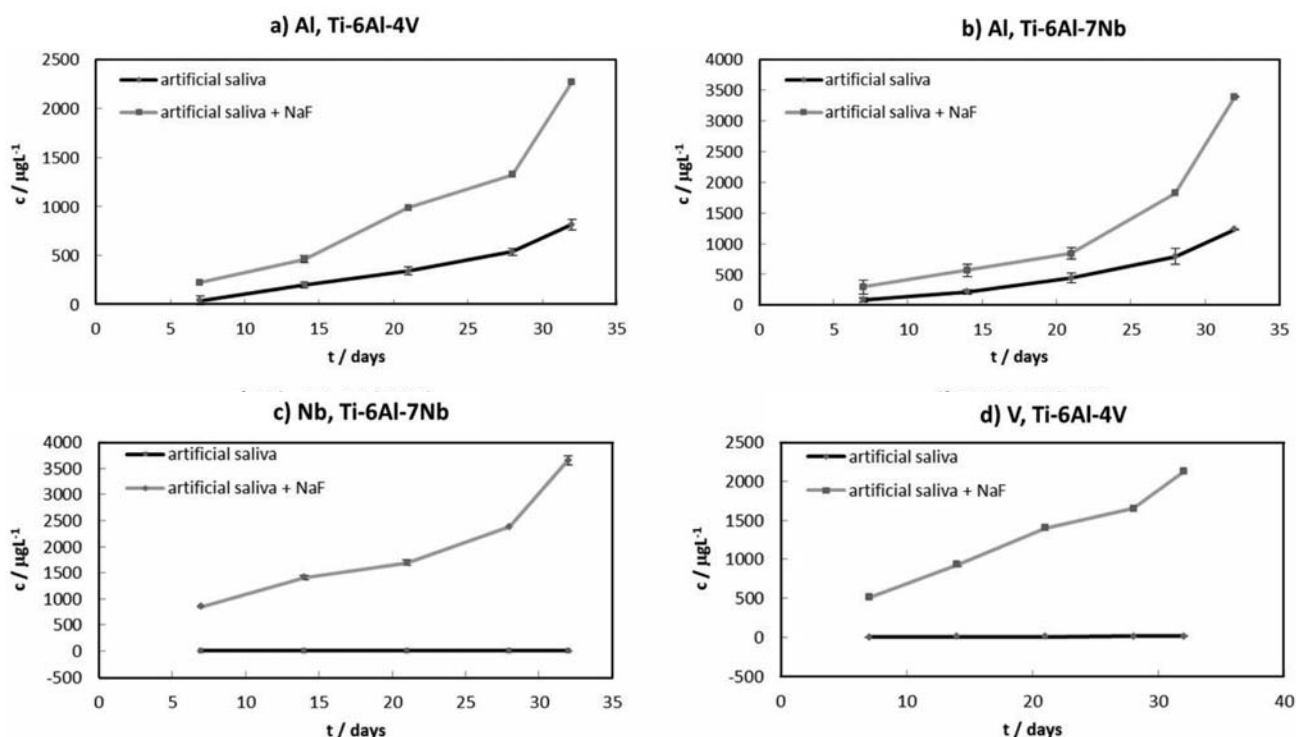


Figure 5. Concentration of (a) aluminium dissolved from Ti–6Al–4V, (b) aluminium dissolved from Ti–6Al–7Nb, (c) niobium dissolved from Ti–6Al–7Nb, and (d) vanadium dissolved from Ti–6Al–4V during 32 days immersion in (a) artificial saliva and (b) artificial saliva containing 0.25% NaF measured by ICP-MS. Symbols and bars represent mean values and standard deviation, respectively. In some cases bars are hardly visible due to small value of standard deviation.

Table 3. Surface composition of the layers formed on Ti, Ti–6Al–7Nb and Ti–6Al–4V during immersion in artificial saliva with and without NaF for 32 days. Composition is deduced based on XPS survey spectra.

Element	Artificial saliva			Artificial saliva + 0.25% NaF		
	Ti	Ti–6Al–7Nb	Ti–6Al–4V	Ti	Ti–6Al–7Nb	Ti–6Al–4V
C	36.2	25.7	34.7	41.2	37.9	57.8
O	47.6	54.2	45.0	43.0	44.7	30.0
Ti	6.7	8.4	6.0	9.7	10.0	6.3
Al	–	2.9	2.6	–	2.2	–
Nb	–	0.4	–	–	0.6	–
V	–	–	–	–	–	0.9
P	3.7	5.0	4.9	1.5	–	–
Ca	2.7	2.7	3.3	1.5	2.0	–
Na	–	0.7	1.0	–	–	–
N	–	–	2.0	–	–	2.5
Cl	–	–	0.5	–	–	–
F	–	–	–	3.1	2.6	2.6

bium (total of 3.3 at. %), whilst the layer formed on Ti–6Al–4V contains only aluminium (2.6 at. %). Consistent with literature data,¹² vanadium was not detected in the oxide layer as it preferentially dissolved into solution due to its poor corrosion resistance (Fig. 2). In addition to oxides the surface layer contains also calcium phosphate (Table 3). The ratio Ca/P ranges between 0.54 and 0.73, i.e. corresponds to the formation of calcium phosphates and not calcium apatites, which exhibit higher Ca/P ratio

(1.67). The major difference in the composition of the surface layer formed during immersion in artificial saliva containing NaF refers to the presence of fluoride in concentrations up to 3.1 at.%. At the same time the concentration of calcium and phosphorus decreases or is diminished.

High resolution XPS spectra enable the chemical differentiation of the elements in the layer. Normalized XPS Ti 2p and O 1s spectra recorded at the surface of Ti, Ti–6Al–7Nb and Ti–6Al–4V after immersion test are de-

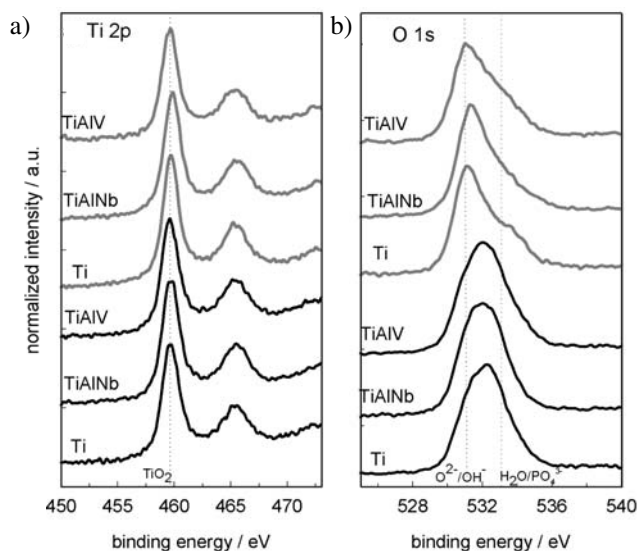


Figure 6. XPS (a) Ti 2p and (b) O 1s spectra recorded at the surface of Ti, Ti–6Al–7Nb and Ti–6Al–4V alloys formed upon immersion for 32 days in artificial saliva (black line) and artificial saliva containing 0.25% NaF (grey line). Dashed lines denote the positions of reference spectra: a) TiO_2 , and b) $\text{O}^{2-}/\text{OH}^-$ and $\text{H}_2\text{O}/\text{PO}_4^{3-}$.

depicted in Fig. 6. The centre of the Ti $2p_{3/2}$ peak is for all samples located at 459.2 eV confirming the presence of titanium(IV) oxide, TiO_2 (Fig. 6a). For the layers formed in artificial saliva the centre of the O 1s spectra is located at approximately 532 eV (Fig. 6b). Since this binding energy is somewhat higher than usually encountered for ox-

ide/hydroxide (531.2 eV), the layer probably comprises also the phosphate component, as oxygen present in phosphate is located at higher binding energy (532.2 eV) than in oxide/hydroxide. In AS+NaF, the peak centre is located at somewhat lower binding energy indicating a smaller amount of phosphate species. As evident from Table 3, the surface layer formed in artificial saliva contains, in addition to oxides, also calcium phosphate. The position of Ca 2p is at about 348.0 eV, in agreement with the position of peaks of $\text{Ca}_8\text{H}_2(\text{PO}_4)_6 \cdot 5\text{H}_2\text{O}$ at 347.2 eV, CaHPO_4 at 347.6 eV, and $\text{Ca}_{10}(\text{PO}_4)_6(\text{OH})_2$ at 347.8 eV.²⁸ The peak related to phosphorus, P 2p, appears at 134.4 eV and can be related to the following compounds: $\text{Ca}_3(\text{PO}_4)_2$ at 132.9 eV, CaHPO_4 at 133.8 eV, and CrPO_4 at 133.4 eV.²⁸

The surface layers formed on Ti–6Al–7Nb and Ti–6Al–4V alloys contain, besides titanium and oxygen, also minor elements aluminium and niobium (Table 3). Normalized XPS Al 2p and Nb spectra recorded at the surface layer formed in artificial saliva are depicted in Fig. 7. For both alloys the position of Al 2p peak at 75.3 eV is consistent with the formation of Al_2O_3 (Fig. 7a). The centre of the Nb 3d peak recorded for the Ti–6Al–7Nb alloy at 208.5 eV is consistent with the formation of Nb_2O_5 (Fig. 7b). Finally, the surface layer formed during immersion in saliva containing fluoride ions contains fluoride (Fig. 7c). The centre of the F 1s is located at 686.2 eV and can be related to the formation of CaF_2 (684.9 eV), Na_2TiF_6 (685.3 eV), K_2TiF_6 (685.0 eV) and Na_3AlF_6 (685.5 eV).²⁸ Therefore, upon immersion in fluoride containing solution the surface layers contain,

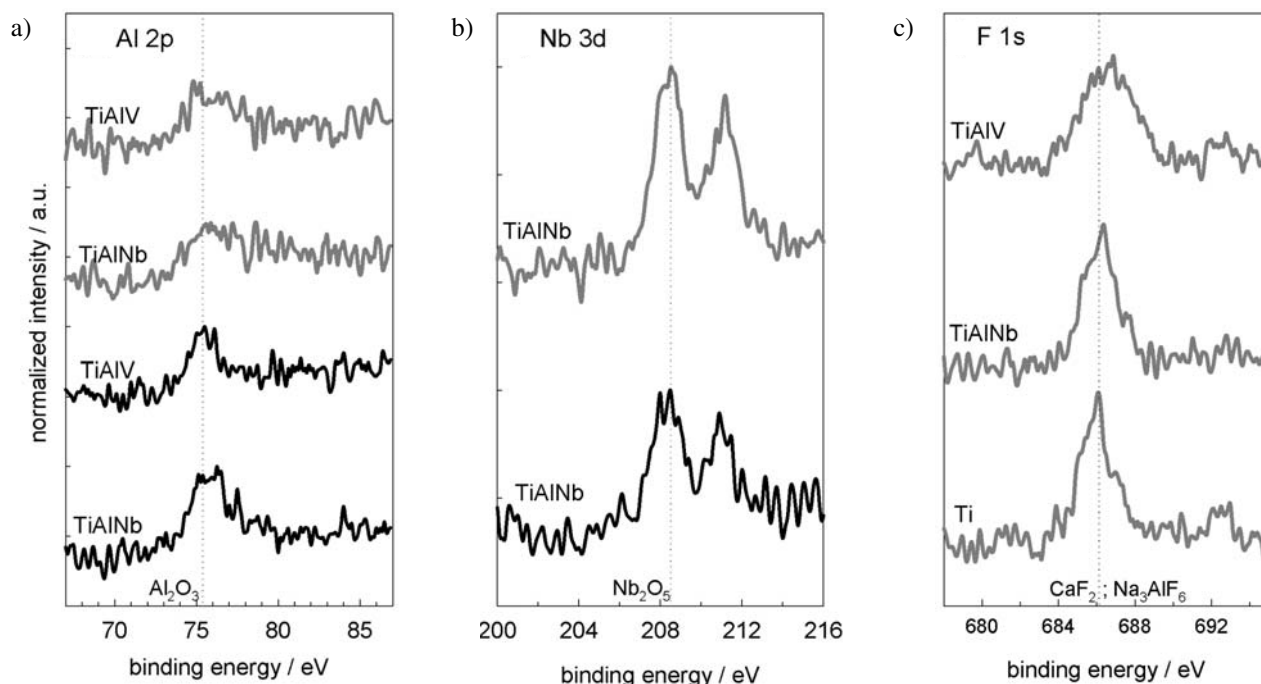


Figure 7. XPS (a) Al 2p, (b) Nb 3d and (c) F 1s spectra recorded at the surface of the layer formed on Ti–6Al–4V and Ti–6Al–7Nb upon immersion for 32 days in artificial saliva (black line) and artificial saliva containing 0.25% NaF (grey line). Dashed lines denote the positions of reference spectra: a) Al_2O_3 , b) Nb_2O_5 and c) CaF_2 and Na_3AlF_6 .

instead of calcium phosphate, calcium fluoride, potassium or sodium hexafluorotitanate and/or hexafluoroaluminate. Several authors noticed that upon immersion in fluoride containing solution the surface layer/product is formed which contains fluorine.^{7,16,19,29} Fluorine was detected in the layer formed upon immersion of titanium for 3 days at 37 °C in 0.9% NaCl containing 0.9% NaF.¹⁶ The authors suggested that compounds like TiF_3 , TiF_4 and/or $TiOF_2$ were formed. These compounds formed because fluoride ions bound to titanium, or titanium oxide, degrade in the solution.¹⁶ Joska and Fojt also identified increased fluorine concentration (48 at.%) in the layer formed on titanium upon 15 minutes immersion in buffered physiological solution containing 5000 ppm F^- .¹⁹ Its presence largely decelerated repassivation during exposure to model saliva. Huang ascribed the presence of fluorine in the layer formed by passivation of the Ti–6Al–4V alloy at 0 V vs. SCE for 2h in acid artificial saliva containing 0.1% NaF to the formation of Ti–F complex compound (Na_2TiF_6).²⁹ In the presence of albumin the titanium surface was protected from the fluoride attack.^{16,29} Stájer *et al.* observed the formation of a strongly bound F-containing complex (Na_2TiF_6).⁷

In-depth composition and thickness of the layers formed on Ti, Ti–6Al–7Nb and Ti–6Al–4V during immersion test are revealed by XPS analysis combined with ion sputtering. Depth profiles are presented in Figs. 8–10. The content of carbon decreased as soon after the sputter process begins, in accordance with its presence as surface contaminant. As the sputter process proceeds and the surface oxide is sputtered away, the content of oxygen progressively decreases, and that of titanium increases (Fig. 8). For alloys, the contents of Al and Nb and V increase as well. Minor elements Ca and P are not well visible on the depth profiles recorded in artificial saliva due to their low concentrations (see Table 3). As a measure of thickness, the sputtering time at which oxygen content decreases to half relative to that at the surface is taken, and then calculated to thickness taken into account the sputtering rate 1.7 nm/min relative to the SiO_2 standard. The estimated thicknesses are presented in Table 4. In the presence of NaF the thickness of the layer increases considerably (Table 4), as evident also in insets with expanded y-scale (Figs. 8c–10c). In the course of immersion fluoride ions are thus incorporated throughout the oxide layer and are not present only at the surface. Despite the increase in thickness, however, the layer formed in fluoride-containing solution is not more corrosion protective, as proved by the electrochemical results (Figs. 1–3). To the best of our knowledge, no data on the effect of fluoride ions on the thickness of the layer formed in artificial saliva is available in the literature based on surface analytical data. Stájer *et al.* reported that, although 10 nm of the of the layer formed on titanium during NaF treatment was removed by Ar^+ bombardment, the XPS F 1s peak at 685.3 eV persisted, proving that the binding between the Ti and

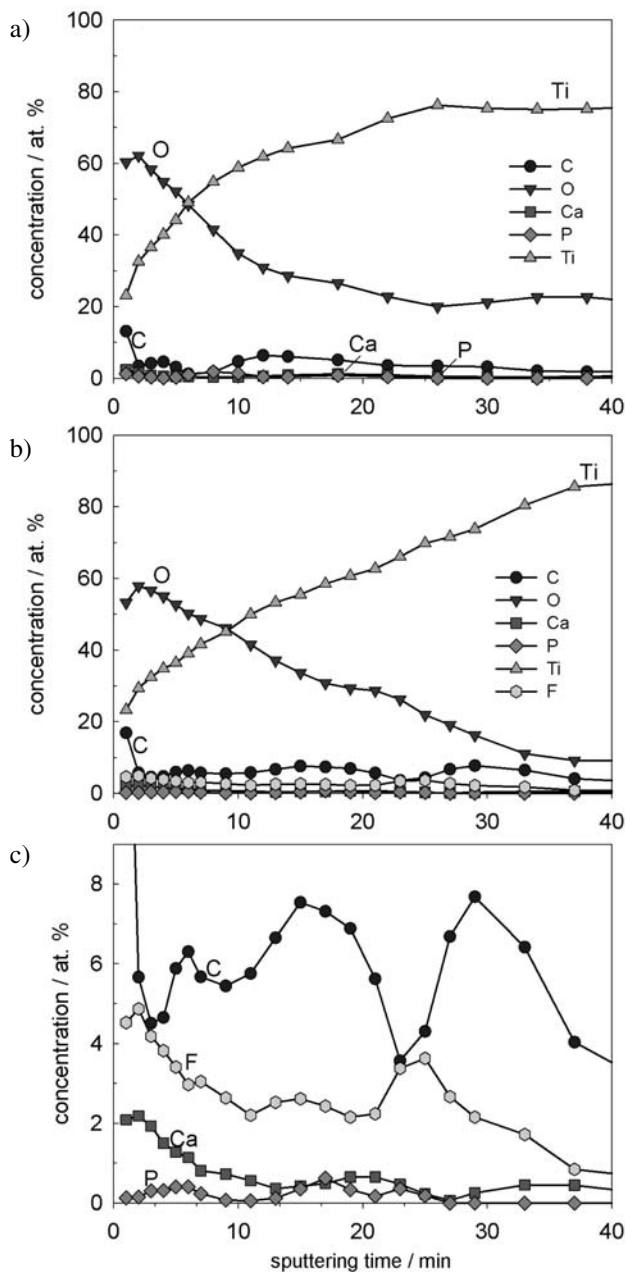


Figure 8. XPS depth profiles of the layers formed on Ti upon immersion for 32 days in (a) artificial saliva (AS) and (b,c) artificial saliva containing 0.25% NaF. Profile in (c) depicts the profile in (b) with expanded y-scale.

F^- was very strong. On the other hand, electrochemical impedance spectroscopy (EIS) data offer data on the resistance and capacitance of the layer formed, and can be explored as an indirect measure of the film thickness. The values of polarization resistance, R_p , decreased to a half by the addition of fluoride ions.^{19,30} With increasing time of immersion the value of R_p gradually increased but even after 50h did not reach the value of the non-fluoride solution.¹⁹ At the same time, the capacitance of the layer decreased.^{19,30} These data are indicative of increasing film thickness, in agreement with the results presented herein.

Therefore, it seems that fluoride ions promote the dissolution of titanium leading to the formation of layer containing titanium, fluorine and oxygen. It seems that this layer is firmly adherent at the surface, and even thicker than the layer formed in the absence of fluoride; however, it is less corrosion protective. The reason may be that this layer is not homogeneous and compact, but rather porous. Indeed, EIS spectra measured in the fluoride containing solution were modelled using a two-layer structure, a dense inner layer and a porous outer porous layer.^{18,19,30} Therefore, the presence of fluoride did not hinder the for-

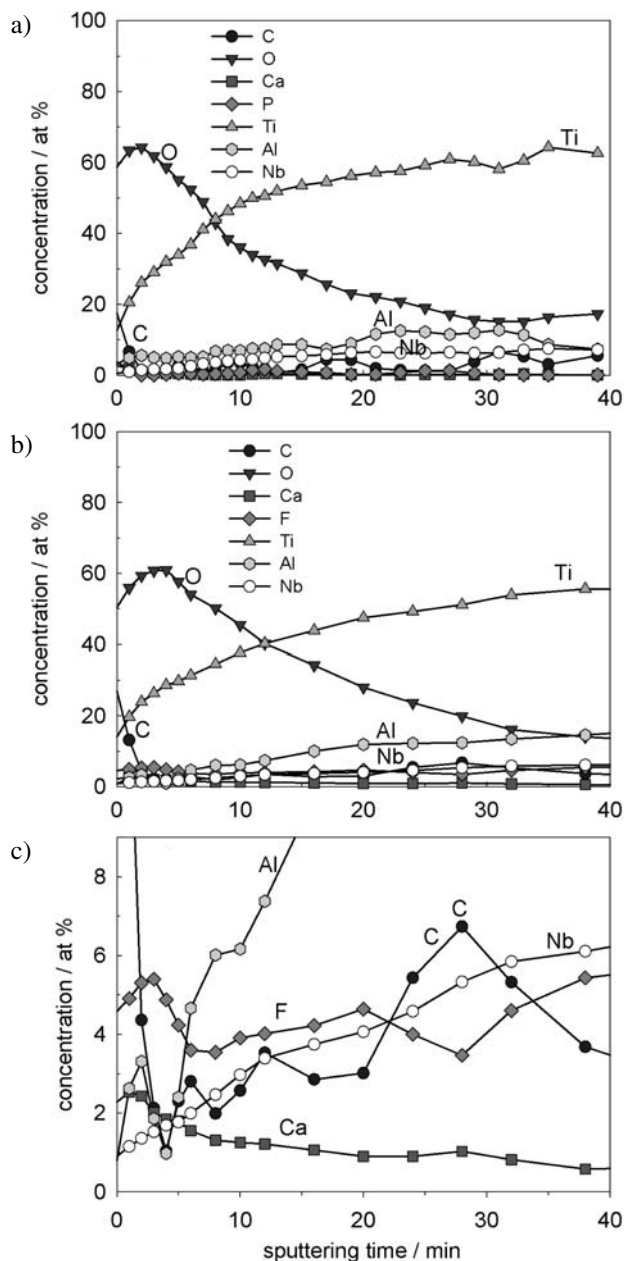


Figure 9. XPS depth profiles of the layers formed on Ti-6Al-7Nb alloy upon immersion for 32 days in (a) artificial saliva (AS) and (b) artificial saliva containing 0.25% NaF. Profile in (c) depicts the profile in (b) with expanded y-scale.

Table 4. Thickness of layers formed on Ti, Ti-6Al-7Nb and Ti-6Al-4V during immersion in artificial saliva with and without NaF for 32 days. Thickness is deduced based on XPS depth profiles in Figs. 8–10.

Material / Solution	Thickness / nm		
	Ti	Ti-6Al-7Nb	Ti-6Al-4V
Artificial saliva	20.4	21.2	20.6
Artificial saliva + 0.25% NaF	35.7	30.6	32.3

mation of oxide layer; instead it influences its composition and properties.

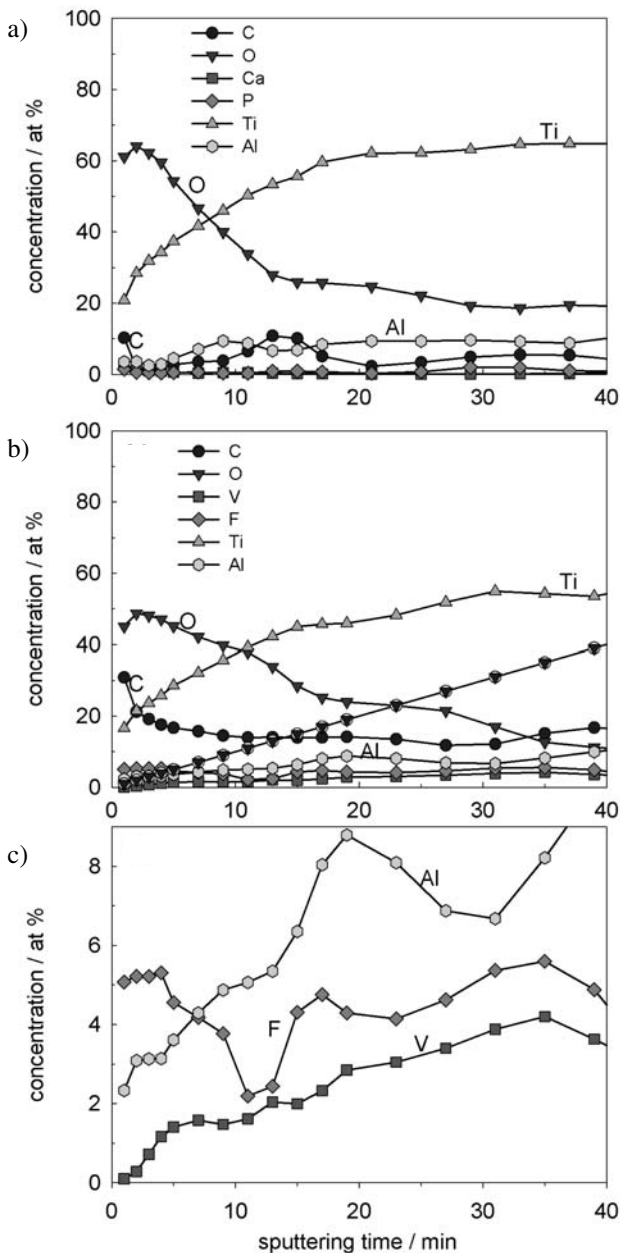


Figure 10. XPS depth profiles of the layers formed on Ti-6Al-4V alloy upon immersion for 32 days in (a) artificial saliva and (b) artificial saliva containing 0.25% NaF. Profile in (c) depicts the profile in (b) with expanded y-scale.

3. 2. 3. Morphology of the Surface

In the solution containing fluoride ions surface exhibits more features related to corrosion than in the absence of fluoride. Example is given for titanium (Figs. 11a,b). These defect features are about 25 μm in width. In the presence of fluoride ions the formation of solid products is noticed at some spots at the surface. These products are formed on Ti, as well as on both alloys. Example is given for the Ti–6Al–4V alloy (Fig. 11c). Their size reaches about 15–20 μm , often being clusters of smaller crystals. The EDS spectra confirm that these crystals correspond to the formation of sodium and/or potassium hexafluorotitanate (Na_2TiF_6 , K_2TiF_6), and sodium and/or potassium hexafluoroaluminate (Na_3AlF_6 , K_3AlF_6) (Figs. 11d,e).

3. 3. Limitation of the Study

In the present study the samples were stationary immersed in artificial saliva with and without addition of sodium fluoride. However, in realistic situation, i.e. as dental implants, material is in fact brushed using toothbrush

three times per day or rinse using mouth water or gel. In recent studies the conditions of brushing and rinsing have been simulated. Fai et al. reported that exposure to toothpastes (i.e. immersion) does not affect titanium *per se*; however, their use during brushing increases roughness of titanium surface.³¹ Khoury et al. used protocol which combined three effects – tooth-brushing, mouthwash rinsing and gel application – to study changes at the surface of one hundred fifty titanium brackets up to 24 months.³² The number and dimension of pits gradually increased due to corrosion with increasing time of testing. A statistical difference was observed for samples tested longer than 18 months. Immersion test up to three days showed that in acetic solution (pH = 3.5) the titanium brackets were severely corroded.³³ Some studies, however, have not detected the detrimental effect of fluoride. Harzer et al. studied corrosion of titanium brackets with fluoride acid toothpaste (pH = 3.2) for 3 minutes, twice per day.³⁴ After 17 months only three brackets three out of 165 brackets tested. It was concluded that the changes were minor and titanium brackets can safely be used.

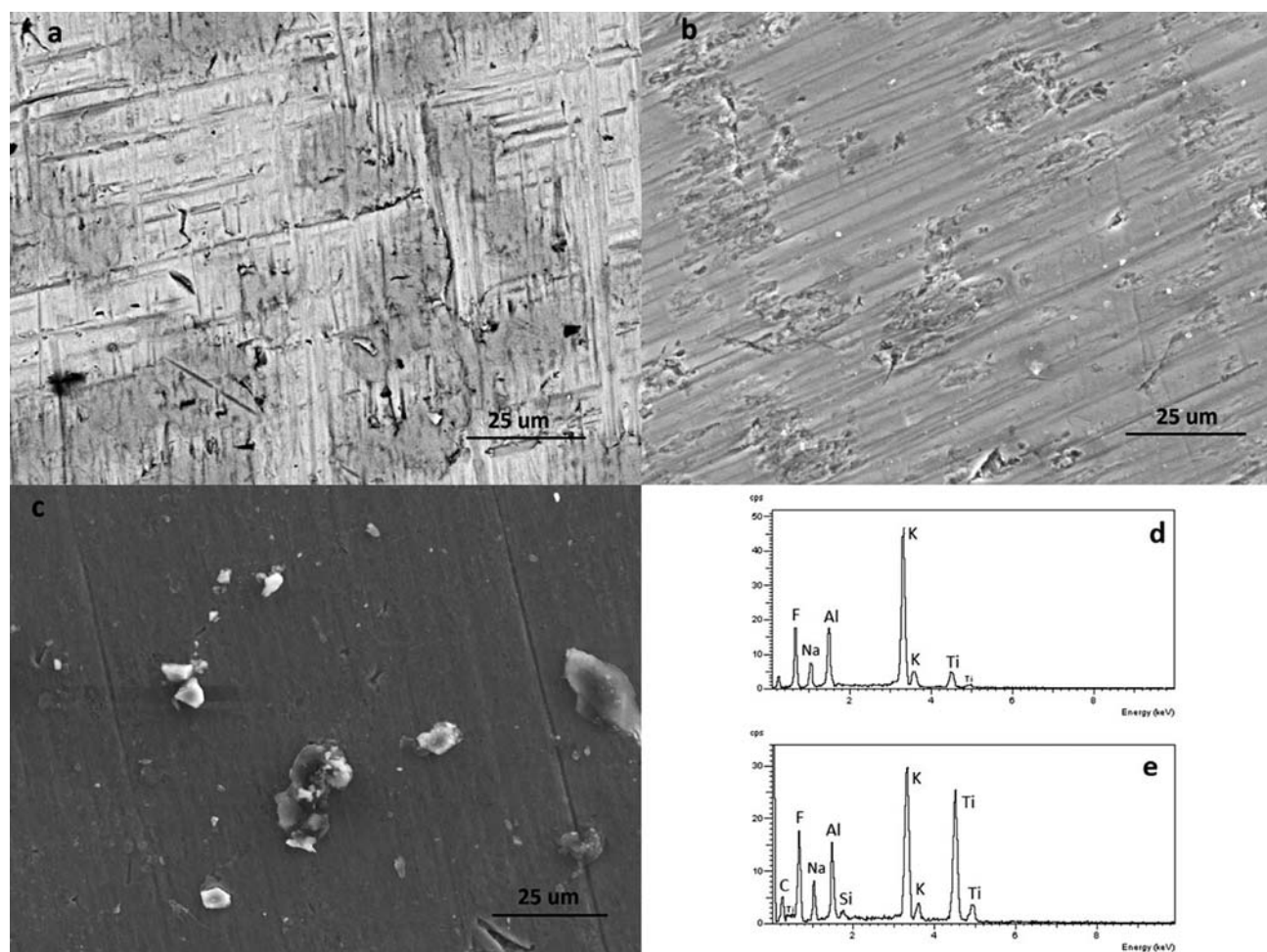


Figure 11. SEM images of Ti after immersion in (a) artificial saliva and (b) artificial saliva containing 0.25% NaF for 32 days. (c) SEM image of crystals formed at the surface of Ti–6Al–4V alloy. (d) EDS spectra of these crystals identified them as Na_2TiF_6 , K_2TiF_6 , Na_3AlF_6 and/or K_3AlF_6 .

4. Conclusions

The corrosion behaviour of three orthopaedic materials, titanium metal, and Ti–6Al–7Nb and Ti–6Al–4V alloys, and their constituent metals has been studied using electrochemical measurements and biodegradation tests in artificial saliva with and without addition of sodium fluoride. In artificial saliva all three Ti-based materials show high corrosion resistance exhibiting a broad passive range due to the formation of passive oxide layer composed mainly of TiO₂. Titanium and Ti–6Al–7Nb alloy exhibit superior behaviour compared to the Ti–6Al–4V alloy. The addition of fluoride strongly affects the electrochemical characteristics: it shifts the corrosion potential in negative direction and increases the current density in the whole potential region.

In artificial saliva titanium, niobium and vanadium are dissolved in low concentrations of few µg/L. On the other hand, aluminium is dissolved in much higher concentrations despite its minor content in the alloy. The addition of fluoride ions increases the dissolution of all metals up to three orders of magnitude. The surface layers formed during biodegradation test are composed mainly of TiO₂. The layer formed on Ti–6Al–7Nb alloy contains also Al₂O₃ and Nb₂O₅, whilst the layer formed on Ti–6Al–4V alloy contains only Al₂O₃ since vanadium is preferentially dissolved and does not contribute to the surface layer. In addition to oxides, the layers formed in artificial saliva contain also calcium phosphate. In the presence of fluoride, the formation of calcium phosphate is diminished. Instead, fluoride is incorporated throughout the depth of oxide layer whose thickness increases compared to that in plain artificial saliva. The layer formed is less protective from that formed in fluoride-free solution. At the surface, calcium fluoride and/or sodium and potassium hexafluorotitanate and hexafluoroaluminate are formed.

This study confirms that the corrosion behaviour of Ti-based alloys is strongly affected by the presence of fluoride ions. In terms of application of these materials for the manufacture of dental or orthodontic implants these facts should be considered. The limitation of the study is, however, that it is a stationary immersion of the materials in artificial saliva containing fluoride while in realistic situation the material is in contact with fluoride several times per day during tooth brushing or mouth rinsing.

5. Acknowledgements

The financial support of this work provided by the Slovenian Research Agency within the research grants J1-2243 and P2-0148 is greatly appreciated. The authors thank Dr. Janez Kovač and Tatjana Filipič, BSc, for XPS measurements.

6. References

1. S. M. Adair, W. H. Bowen, B. A. Burt, J. V. Kumar, S. M. Levy, D. G. Pendrys, R. G. Rozier, R. H. Selwitz, J. W. Stamm, G. K. Stookey, G. M. Whitford, Recommendations for Using Fluoride to Prevent and Control Dental Caries in the United States, <http://www.cdc.gov/mmwr/>.
2. M. Ponikvar, in: A. Tressaud, G. Haufe (Ed.): Fluorine and Health, Elsevier, **2008**, pp. 488–549.
3. T. Aoba, *Crit. Rev. Oral Biol. Med.*, **1997**, *8*, 136–153.
4. W. Geurtsen, *Crit. Rev. Oral Biol. Med.*, **2002**, *13*, 71–84.
5. C. Manaranche, H. Hornberger, *Dental Mater.*, **2007**, *23*, 1428–1437.
6. D. G. Olmedo, M. L. Paparella, D. Brandizzi, R. L. Cabrini, *Int. J. Oral Maxillofac. Surg.*, **2010**, *39*, 503–507.
7. A. Stájer, K. Ungvári, I. K. Pelsöczy, H. Polyánka, A. Oszkó, F. Mihalik, Z. Rakonczay, M. Radnai, L. Kemény, A. Fazekas, K. Turzó, *J. Biomed. Mater. Res. A*, **2008**, 450–458.
8. E. Blažević, I. Milošev, *Vakuumist*, **2007**, *27*, 20–23.
9. K. Elagli, M. Traisnel, H. F. Hidebrand, *Electrochim. Acta*, **1993**, *38*, 1769–1774.
10. The European directive restricting the use of nickel, <http://www.teg.co.uk/nickel/94-27-EC.htm>.
11. J. A. Disegi, *Injury*, **2000**, *31*, S-D14–17.
12. I. Milošev, M. Metikoš-Huković, H.-H. Strehblow, *Biomaterials*, **2000**, *21*, 2103–2113.
13. I. Milošev, T. Kosec, H.-H. Strehblow, *Electrochim. Acta*, **2008**, *53*, 3547–3558.
14. T.-H. Lee, C.-C. Wang, T.-K. Hunag, L.-K. Chen, M.-Y. Chou, H.-H. Huang, *J. Alloys Compd.*, **2009**, *488*, 482–489.
15. N. Schiff, B. Groszogeat, M. Lissac, F. Dalard, *Biomaterials*, **2002**, 1995–2002.
16. S. Takemoto, M. Hattori, M. Yoshinari, E. Kawada, Y. Oda, *Biomaterials*, **2005**, *26*, 829–837.
17. H.-H. Huang, T.-H. Lee, *Dental Mater.*, **2005**, *21*, 749–755.
18. A. Robin, J. P. Meirelis, *Mater. Corros.*, **2007**, *58*, 173–180.
19. L. Joska, J. Fojt, *J. Mater. Sci. Mater. Med.*, **2010**, *21*, 481–488.
20. F. Toumelin-Chemla, F. Rouelle, G. Burdairon, *J. Dentistry*, **1996**, *24*, 109–115.
21. Z. Cai, H. Nakajima, N. Woldu, A. Berglund, M. Bergman, *Biomaterials*, **1999**, *20*, 183–190.
22. H. H. Uhlig, R. Winstone Revie, Corrosion and Corrosion Control, Third edition, John Wiley & Sons, 1985.
23. <http://www.rbdinstruments.com>
24. M. Metikoš-Huković, A. Kwokal, J. Piljac, *Biomaterials*, **2003**, *24*, 3765–3775.
25. I. Milošev, D. Blejan, S. Varvara, L. M. Muresan, *J. Appl. Electrochem.*, **2013**, *43*, 645–658.
26. N. Kovačević, B. Pihlar, V. S. Šelih, I. Milošev, *Acta Chim. Slov.* **2012**, *59*, 144–155.
27. I. Milošev, *Pure Appl. Chem.*, **2011**, *83*, 309–324.
28. NIST X-ray Photoelectron Spectroscopy Database, NIST Standard Reference Database 20, Version 3.5, Data compiled and evaluated by C. D. Wagner, A. V. Naumkin, A. Kraut-Vass, J. W. Allison, C. J. Powell, J. R. Rumble, Jr., <http://>

- srdata.nist.gov/xps/.
29. H.-H. Huang, *Biomaterials*, **2003**, *24*, 275–282.
30. A. M. Al-Mayouf, A. A. Al-Swayih, N. A. Al-Mobarak, A. S. Al-Jabab, *Mater. Chem. Phys.*, **2004**, *86*, 320–329.
31. L. M. G. Fais, R. B. Fernandes-Filho, M. A. Pereira-da-Silva, L. G. Vaz, G. L. Adabo, *J. Dentistry*, **2012**, *40*, 265–275.
32. E. S. Kuoury, M. Abboud, N. Bassil-Nassif, J. Bouserhal, *Int. Orthodontics*, **2011**, *9*, 432–445.
33. H.-H. Kang, S.-B. Park, H.-I. Kim, Y.-H. Kwon, *Dental Mater. J.*, **2008**, *27*, 555–560.
34. W. Harzer, A. Schröter, T. Gedrange, F. Muschter, *Angle Orthodontist*, **2001**, *71*, 318–323.

Povzetek

Kovinski materiali, ki jih uporabljamo za izdelavo zobnih vsadkov ali pripomočkov, morajo izkazovati visoko korozijsko odpornost. Ustna votlina je za kovino agresivni medij, saj predstavlja večkomponentno okolje z širokim razponom različnih pogojev, ki obsegajo velike spremembe temperature, vrednosti pH, prisotnost bakterij in tudi pogoje abrazije. Zaradi povečane uporabe materialov na osnovi titana za izdelavo zobnih vsadkov in ortodontskih pripomočkov se postavlja vprašanje korozijske odpornosti teh materialov v prisotnost fluoridnih ionov, ki so dodani zobnim pastam in različnim gelom in ustnih vodah. Korozijsko obnašanje kovine Ti in dveh njegovih zlitin, Ti–6Al–7Nb in Ti–6Al–4V, ter posameznih kovinskih komponent, smo raziskovali v umetni slini z in brez dodatka fluoridnih ionov. Le-ti močno vplivajo na korozijski proces in povečujejo raztapljanje kovine, kar smo pokazali z metodo elektrokemijske polarizacije. Izvedli smo tudi test potapljanja v trajanju 32 dni. Med tem časom smo merili koncentracijo kovinskih ionov z masno spektroskopijo s sklopljeno induktivno plazmo. Po koncu test smo sestavo, debelino in morfologijo plasti na površini analizirali z rentgensko fotoelektronsko spektroskopijo in vrstično elektronsko mikroskopijo.